

THE OPTICAL PROPERTIES OF p -TYPE Bi_2Te_3 - Sb_2Te_3 ALLOYS BETWEEN 2-15 MICRONS

R. SEHR and L. R. TESTARDI

The Franklin Institute Laboratories, Philadelphia, Pennsylvania

(Received 19 February 1962)

Abstract—Transmittance and reflectance measurements have been made on a number of p -type Bi_2Te_3 - Sb_2Te_3 alloys. With the electric vector in the cleavage plane, the index of refraction, energy gap, and average effective mass have been calculated. The absorption edge indicates indirect transitions but the analysis based on phonons of a single energy is inconsistent. The reduction of the dielectric constant due to the free carrier susceptibility is observed in the alloys. In contrast to thermal energy gaps the optical energy gaps increase with increasing Sb content, a result attributed in part to the increasing degeneracy of the charge carriers. Temperature dependencies of the optical energy gaps are also reported.

INTRODUCTION

THE TRANSPORT properties of Bi_2Te_3 and its alloys with Sb_2Te_3 have been investigated in considerable detail in recent years.* In part, these studies have yielded information of immediate interest for the application of these materials in thermoelectric devices operating near room temperature. The infrared optical properties of Bi_2Te_3 have been investigated by AUSTIN^(1, 2) and the optical energy gaps of the pure compounds have been reported by BLACK *et al.*,⁽³⁾ but it appears that no work on the alloy compositions has been published.

From transmittance and reflectance measurements we have sought to determine the compositional dependence of the energy gap, the index of refraction, and the average effective mass of the holes obtained from free carrier absorption and electric susceptibility. In principle the experimental results may provide some information on the band structure but the analysis of the absorption edge has failed to provide a consistent interpretation. The degeneracy of the charge carriers may be partially responsible for this.

SAMPLE PREPARATION

The p -type single crystals used in this work were grown by zone melting in a soft mold (see

previous paper). Samples for optical measurements were taken from the central portions of the ingots.† For reflectance measurements the specimens were cleaved to yield, over the measured area, a mirrorlike surface with no visible stepping. Samples for transmission measurements were taken from the cleavage face of the reflectivity specimens. The sample thickness was found from mass and area measurements and the known density of the alloy compositions.⁽⁴⁾ In the absence of visible stepping the uniformity of the thickness determined by interference fringes and sectioned sample density measurements was found adequate.

MEASUREMENTS

Room temperature reflectance and transmittance measurements were made on a Perkin Elmer Model 21 double beam spectrometer. For low temperature transmittance measurements the single beam Model 12B with the light chopped at the source was used to avoid the wavelength dependent zero shift due to temperature differences between the sample and detector. Sample thicknesses between 4 and 12 microns were used to obtain appreciable transmission losses from absorption ($Kd \geq 1$,

† The optical samples came from the same ingots as did the samples on which the transport properties, reported in the preceding paper, were measured.

* See previous paper for partial list of references.

with K , the absorption coefficient and d the sample thickness) while retaining a transmitted intensity of measurable magnitude.

Reflectance measurements were made at an angle slightly off normal incidence on the cleavage face of a thick specimen so that internally reflected radiation did not contribute to the observed intensity. From Fresnel's equations the slightly off normal angle of incidence generally was found to contribute a negligible error in the use of the reflectivity equation for normal incidence. The reflectance of the samples was measured relative to an aluminum reference mirror whose absolute reflectance has been reported elsewhere.⁽⁵⁾

If the interference fringes are not resolved the extinction coefficient, k , and the index of refraction, n , are obtained from the transmittance, T , the reflectance, R , and the sample thickness, d , by⁽⁶⁾

$$T = (1 - R)^2 e^{-Kd} / (1 - R^2 e^{-2Kd}) \quad (1)$$

and

$$R = \frac{(n-1)^2 + k^2}{(n+1)^2 + k^2} \quad (\text{normal incidence}), \quad (2)$$

with the absorption coefficient $K = 4\pi k/\lambda$. At low temperatures the reflectances were not measured and the absorption coefficient was obtained from transmission measurements on two samples of different thicknesses. In this case, to a fair approximation, K can be obtained by neglecting the second term in the denominator of equation (1).

RESULTS

The reflectances, R_B for Bi_2Te_3 and R_S for Sb_2Te_3 are given in Fig. 1. Both initially decline with increasing wavelength due to the decrease in the refractive index, but for Sb_2Te_3 the reflectance reaches a minimum around 9 microns and rises steeply thereafter to metallic values. This is the consequence of increasing free carrier absorption. Upon substitution of Bi for Sb in Sb_2Te_3 this minimum shifts to longer wavelengths.

The index of refraction for various alloy compositions (indicated by the mol per cent Sb_2Te_3) is given as a function of wavelength in Fig. 1. In the long wavelength region, n was obtained from equation (2) while at the shorter wavelengths more accurate values were obtained from the

interference fringes by the relation

$$2nd = N\lambda$$

where N is the order of interference. An approximate value for N was first obtained from equation (3) using the value for n obtained with equation (2).

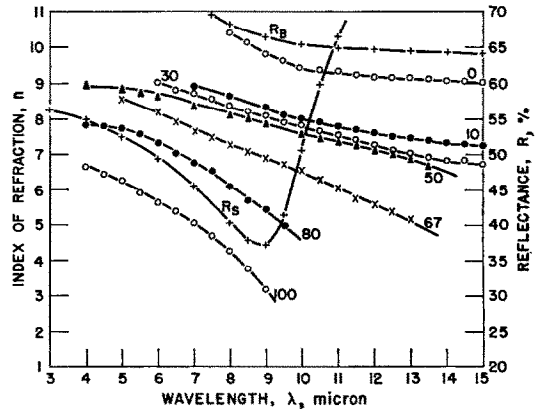


FIG. 1. Reflectance (R_B for Bi_2Te_3 and R_S for Sb_2Te_3) and index of refraction, n , for various alloy compositions.

With the nearest integer taken as the correct value for N , equation (3) was applied to successive fringe maxima to obtain the dispersion more accurately. These results generally agreed to within five per cent with the values for n obtained from reflectance and transmittance measurements.

The refractive index at a given wavelength decreases with increasing Sb content. The large value of n for Bi_2Te_3 has been reported earlier by AUSTIN.⁽¹⁾

SPITZER and FAN⁽⁷⁾ have shown that the contribution from the free carrier electric susceptibility to the real dielectric constant ϵ , can be written

$$\epsilon = \epsilon_i - \frac{Ne^2 \cdot \lambda^2}{4\pi^2 c^2 \epsilon_0 m_\chi^*} = n^2 - k^2 \quad (4)$$

where ϵ_0 and ϵ_i are the dielectric constants for free space and for the material in the absence of carriers respectively, N is the carrier concentration, and m_χ^* is the electric susceptibility effective mass. In Fig. 2 the real dielectric constant ϵ is plotted vs. λ^2 . Equation (4) is well followed at the longer wavelengths (assuming ϵ_i to be wavelength independent) while at the shorter wavelengths the

experimental results deviate from the λ^2 behavior due to the approaching absorption edge. The dielectric constants of the intrinsic alloys appear to be relatively large for all compositions although smaller than the value for Bi₂Te₃. The electric susceptibility from the large carrier concentrations for the alloys in the as-grown state leads to a smaller and wavelength dependent, dielectric constant in the near infrared. No simple correlation

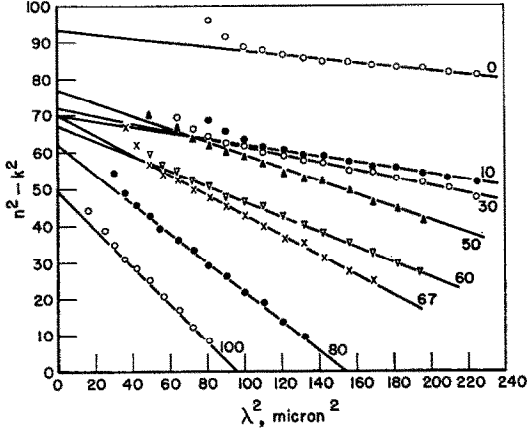


FIG. 2. The real dielectric constant $\epsilon = n^2 - k^2$ vs. λ^2 for various alloy compositions.

between the reduction of the dielectric constant and the compositional dependence of the Hall mobilities was indicated.

From the slope of ϵ vs. λ^2 , in Fig. 2, m^* may be calculated. For the many valley model proposed for the band structure of Bi₂Te₃^(8,9) m_x^* is identical with the inertial effective mass in the cleavage planes and is given as α_1^{-1} in AUSTIN's notation.⁽¹⁰⁾ However, the carrier concentrations were not known and N was replaced by the measured Hall coefficient, R_H , using

$$R_H = \left(\frac{\alpha_3'}{\alpha_1^2} \right) \cdot \frac{\langle \tau^2 \rangle}{\langle \tau \rangle^2} \cdot \frac{1}{Ne} \quad (5)$$

The quantity (α_3'/α_1^2) is the Hall coefficient anisotropy factor. The relaxation time averages were calculated using the scattering law and Fermi levels determined from the transport properties (see previous paper). With equations (4) and (5) the effective mass parameter (α_1/α_3') can be calculated from the free carrier electric susceptibility.

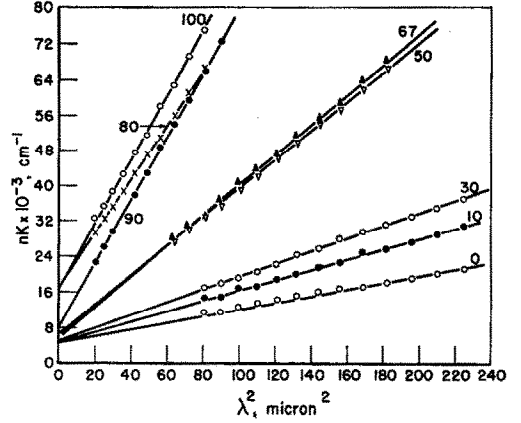


FIG. 3. Product of index of refraction and absorption coefficient, nK vs. λ^2 for various alloy compositions.

The compositional dependence of (α_1/α_3') at 300°K is given in Fig. 4.

The same effective mass parameter evolves from the absorption coefficient measurements. With the electric vector in the cleavage planes the free carrier absorption coefficient, K is given by⁽¹⁰⁾

$$K = \frac{e^2 \lambda^2}{4\pi^2 n \epsilon_0 m^2 c^3 \mu_H R_H} \left(\frac{\alpha_1}{\alpha_3'} \right)_A^2 \cdot \left(\frac{\langle \tau^2 \rangle}{\langle \tau \rangle^2} \right) \times \langle \tau \rangle \cdot \langle \tau^{-1} \rangle, \quad (6)$$

where μ_H is the Hall mobility. The plot of nK for eight compositions, given in Fig. 3, shows that the desired λ^2 dependence of the free carrier absorption

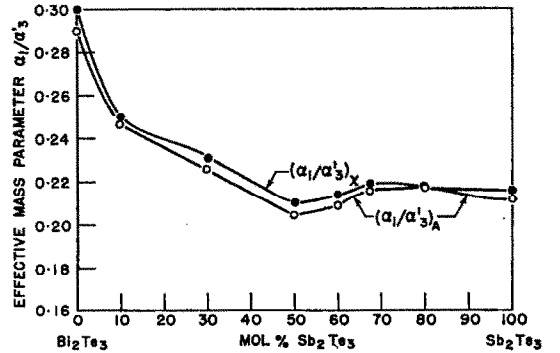


FIG. 4. The effective mass parameter α_1/α_3' determined from free carrier susceptibility, $(\alpha_1/\alpha_3')_x$ and from free carrier absorption, $(\alpha_1/\alpha_3')_A$ vs. composition.

is superimposed on a broad band absorption component of undetermined origin. The effective mass parameter $(\alpha_1/\alpha_3)_A$ obtained from equation (6) and the slopes in Fig. 3 are plotted as a function of composition in Fig. 3. The agreement between $(\alpha_1/\alpha_3)_A$ and $(\alpha_1/\alpha_3)_X$ which was obtained principally from reflectance measurements is to within five per cent. The values for Bi_2Te_3 are in agreement with Austin's results obtained from free carrier absorption and Faraday rotation measurements.

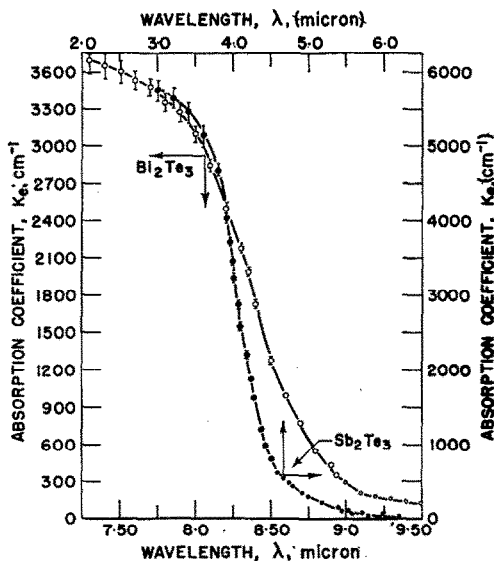


FIG. 5. Absorption coefficient, K_e , due to band to band transitions vs. λ for Bi_2Te_3 and Sb_2Te_3 .

With the free carrier and broad band absorption components subtracted the remaining absorption coefficient K_e was analyzed to obtain the optical energy gap and characterize the transition as direct or indirect. In Fig. 5 K_e is plotted as a function of wavelength for the two extreme compositions of the alloy system. In determining the energy gap E_g we have followed Moss' criterion⁽¹¹⁾ which establishes E_g from the value of λ at which the slope of the absorption coefficient is a maximum. Fig. 6 gives the energy gap as a function of composition for three different temperatures. From Bi_2Te_3 to 80 per cent Sb_2Te_3 /20 per cent Bi_2Te_3 the energy gap increases linearly with Sb_2Te_3 content. The temperature coefficient of E_g is approximately

$1.5 \times 10^{-4} \text{ eV}/^\circ\text{K}$ in this range of composition, although from the increased degeneracy at the lower temperatures a somewhat smaller value would be expected for intrinsic material.⁽²⁾ For the very Sb rich alloys E_g rises sharply to about 0.28 eV for Sb_2Te_3 at room temperature. For these compositions the Fermi level is almost independent of the temperature and a smaller temperature coefficient of E_g will be expected. Since intrinsic and n -type specimens of the Sb rich alloys generally cannot be obtained an accurate determination

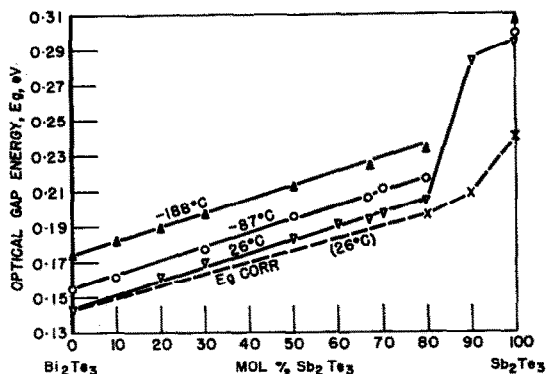


FIG. 6. Optical energy gap, E_g , vs. composition.
 $E_{g \text{ corr}} = E_g (\text{observed}) - \text{Fermi energy}$

of the effects of degeneracy was not possible. At least in part the increase in E_g with increasing Sb_2Te_3 content results from the increase in the as-grown state of degeneracy and is similar to the situation found in InSb .⁽¹²⁾ An estimate of this was provided by calculating the Fermi level, E_F , from the observed Seebeck coefficient. The results have been plotted in Fig. 6 as $E_{g \text{ corr}} = E_g - E_F$. If the transitions were direct an additional increase in E_g would be associated with the ratio of the density of states effective masses for the holes and electrons. The bulk of the experimental evidence, however, indicates indirect transitions.

The absorption edges of several alloys were analyzed to determine whether the transitions were direct or indirect. Generally, $K_e \propto (h\nu - E_g)^n$ where $h\nu$ is the incident photon energy and $n = \frac{1}{2}$ or $\frac{3}{2}$ for direct transitions and $n = 2$ or 3 for indirect transitions. Our data are consistent with $n = 2$ as shown in Fig. 7 for Bi_2Te_3 and Sb_2Te_3 . In both cases the plot of $K_e^{1/2}$ vs. $h\nu$ breaks into

two straight lines as predicted for indirect transitions by the expression of MACFARLANE and ROBERTS.⁽¹³⁾

$$K_e = A \left[\frac{(h\nu - E_g - k\theta)^2}{1 - \exp(-\theta/T)} + \frac{(h\nu - E_g + k\theta)^2}{\exp(\theta/T) - 1} \right] \quad (7)$$

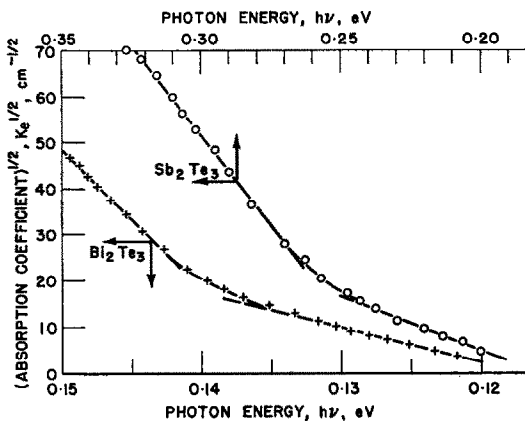


FIG. 7. Square root of absorption coefficient, $K_e^{1/2}$, vs. incident photon energy for Bi₂Te₃ and Sb₂Te₃.

where $k\theta$ is the phonon energy necessary to conserve momentum. The first term corresponds to phonon emission and the second to phonon absorption. Applying this equation to our results at room temperature we obtain from the intercepts $k\theta$ equal to 150°K and 400°K and E_g equal to 0.13 eV and 0.21 eV for Bi₂Te₃ and Sb₂Te₃ respectively. The corresponding values of $k\theta$ from the slopes, however, are about three and four times larger, respectively. A similar discrepancy for Bi₂Te₃ has been reported by AUSTIN.⁽¹⁾ Although equation (7) does not account for degeneracy this should be unimportant in Bi₂Te₃. Ignoring the modification of equation (7) by degeneracy the optical energy gaps computed for indirect transitions from the intercepts of Fig. 7 are smaller than those obtained by Moss' criterion (Fig. 6). This result, together with the effects of degeneracy, will account at least in part for the apparent discrepancy between optical and thermal energy gaps. Values for the thermal energy gaps from high temperature resistivity measurements have been obtained in this laboratory. The results show an energy gap of 0.15 eV for Bi₂Te₃ which decreases on alloying to about 0.1 eV at 70 per cent Sb₂Te₃/30 per cent

Bi₂Te₃. With increasing degeneracy our optical and thermal measurements would tend, respectively, to overestimate and underestimate the energy gap. For the very Sb rich compositions (including Sb₂Te₃) the strong degeneracy led to resistivity maxima at temperatures too close to the melting points to permit a determination of E_g . Attempts at compensation were unsuccessful.

CONCLUSIONS

The infrared studies have shown that most of the alloy system is characterized by a large dielectric constant although the effects of the free carrier susceptibility are quite marked for the more degenerate alloys. For the larger part the optical behavior was in agreement with the predictions of the Drude-Zener theory. An effective mass average obtained from electric susceptibility and free carrier absorption measurements is reported but more work is needed to establish the band structure parameters completely.

Evidence obtained from measurements of the transport properties indicate the effective mass to be insensitive to variations in carrier concentration or degeneracy, at least over changes in these two variables as occur in the as-grown materials. Although exact carrier concentrations cannot be obtained from Hall measurements without further knowledge of the band structure, it is estimated that a hole concentration in excess of 10^{19} cm⁻³ occurred in most of the alloys. A possible reason for independence of the effective mass on hole concentration at such levels seems to be the very large dielectric constant screening of the crystalline field. In a calculation for heavily doped Germanium CONWELL and SCHLOSSER⁽¹⁴⁾ arrive at a similar conclusion.

In the analysis of the absorption edge the transitions appear as indirect but no satisfactory account was made of the effects of degeneracy. At least in the compositional range Bi₂Te₃ to 70 per cent Sb₂Te₃/30 per cent Bi₂Te₃ the energy gap should fall somewhere between the optical and thermal values and, therefore, does not vary to a great extent with composition.

Acknowledgements—The authors wish to thank Mr. G. K. McCONNELL for his valuable aid in the experimental work and the sponsors of the Thermoelectric Effects Research Program for their financial support.

REFERENCES

1. AUSTIN I. G., *Proc. phys. Soc. Lond.* **72**, 545 (1958).
2. AUSTIN I. G., *Proc. phys. Soc. Lond.* **76**, 169 (1960).
3. BLACK J., CONWELL E. M., SEIGLE L. and SPENCER C. W., *J. Phys. Chem. Solids* **2**, 240 (1957).
4. TESTARDI L. R. and WIESE J. R., *Trans. Amer. Inst. min. (metall.) Engrs.* **221**, 646 (1961).
5. HASS G., *J. opt. Soc. Amer.* **45**, 945 (1955).
6. BECKER M. and FAN H. Y., *Phys. Rev.* **76**, 1530 (1949).
7. SPITZER W. G. and FAN H. Y., *Phys. Rev.* **106**, 882 (1957).
8. DRABBLE J. R. and WOLFE R., *Proc. phys. Soc. Lond.* **B69**, 1101 (1956).
9. DRABBLE J. R., *Proc. phys. Soc. Lond.* **72**, 380 (1958).
10. AUSTIN I. G., *J. Electron. Cont.* **6**, 271 (1959).
11. MOSS T. S., *Optical Properties of Semiconductors*, p. 40. Academic Press, New York (1959).
12. BURSTEIN E., *Phys. Rev.* **93**, 632 (1954).
13. MACFARLANE G. G. and ROBERTS V., *Phys. Rev.* **97**, 1714 (1955).
14. CONWELL E. M., SCHLOSSER H., *Bull. Amer. phys. Soc.* **7**, 214 (1962).